Explicit Upwind Schemes for Lossy MTL's with Linear Terminations

Joe LoVetri and Tibor Lapohos

***Abstract*—The time domain multiconductor transmission line (MTL) equations are written as a general first order system of partial differential equations and a characteristic decomposition is used to obtain first order and second order accurate upwind differencing schemes. Linear boundary conditions in the form of generalized *Thévenin* equivalent sources are incorporated into the scheme. These schemes are compared with the standard time-space centered second order accurate leapfrog scheme where the current and voltage variables are interlaced in space and time. For any general explicit numerical scheme, for a given MTL, only the fastest propagating TEM mode can be solved for at the *Courant* limit of the scheme. This causes the other slower modes to disperse. The results of our comparisons, show that at the *Courant* number both upwind schemes produce less numerical dispersion for the slower propagating modes than the standard leapfrog scheme under the same conditions. In addition, the *Courant* number of the second order upwind scheme is twice that of the leapfrog scheme. These advantages make the upwind schemes better tools to model inhomogeneous MTL's with linear terminations.**

***Index Terms*—Boundary value problem, initial value problem, leapfrog, MTL, upwind differencing.**

I. Introduction

THE EQUATIONS describing the quasi-TEM mode of propagation [1] in multiconductor transmission lines consisting of $M+1$ lines can be represented as

$$\begin{cases} L\mathbf{i}_t + R\mathbf{i} + \mathbf{v}_x = \mathbf{v}_f \\ C\mathbf{v}_t + G\mathbf{v} + \mathbf{i}_x = \mathbf{i}_f \end{cases} \tag{1}$$

where R, G, L, C are the $M \times M$ per unit length resistance, conductance, inductance, and capacitance parameter matrices, respectively, $\mathbf{v}(x,t)$ and $\mathbf{i}(x,t)$ are the line voltage and current vectors whereas $\mathbf{v}_f(x,t)$ and $\mathbf{i}_f(x,t)$ are the per unit length source terms representing the incident electromagnetic field coupling (subscripts t and x denote differentiation with respect to those variables).

Although important from a physical point of view [2], [3], the frequency-dependence of the losses is neglected and only DC type losses are considered in this paper. The reason for this is to ease the design of the numerical schemes and make possible a good understanding of their properties. The addition of frequency-dependent losses should be straightforward [4]. Furthermore, the lines are assumed *time invariant* and *uniform with respect to* x, hence the parameter matrices are constant. We also assume that the MTL is perfectly shaded from any external electromagnetic field and thus $\mathbf{v}_f$ and $\mathbf{i}_f$ are zero. All schemes presented herein can be extended, in a simple way, to the case of nonzero external field.

The boundary conditions are represented as generalized *Thévenin* sources with internal resistance matrices R_{Tn} and R_{Tf} for the near- and far-end, respectively. The *Thévenin* voltage sources are specified as $\mathbf{v}_{Tn}(t)$ and $\mathbf{v}_{Tf}(t)$. Based on Kirchhoff's and Ohm's law, we can write

$$\mathbf{v}_0 + R_{Tn}\mathbf{i}_0 = \mathbf{v}_{Tn} \tag{2}$$

$$\mathbf{v}_N - R_{Tf}\mathbf{i}_N = \mathbf{v}_{Tf}. \tag{3}$$

The partial differential equations in (1), together with boundary conditions (2) and (3), have been previously solved using a time-space centered second order accurate leapfrog scheme where the location of the discretized current vector is interlaced with the location of the discretized voltage vector in both time and space [5], [6].

Thus, letting $\mathbf{i}_{j+1/2}^{n+1/2} \approx \mathbf{i}((j+1/2)\Delta x, (n+1/2)\Delta t)$ and $\mathbf{v}_j^n \approx \mathbf{v}(j\Delta x, n\Delta t)$ represent the interlaced current and voltage vectors on an MTL which is discretized in N cells of length Δx, the leapfrog update equations are written as

$$\mathbf{i}_{j+1/2}^{n+1/2} = \left(\frac{L}{\Delta t} + \frac{R}{2}\right)^{-1}\left[\left(\frac{L}{\Delta t} - \frac{R}{2}\right)\mathbf{i}_{j+1/2}^{n-1/2} - \frac{1}{\Delta x}\left(\mathbf{v}_{j+1}^n - \mathbf{v}_j^j\right) + \frac{1}{2}\left(\mathbf{v}_{f_{j+1/2}}^{n+1/2} + \mathbf{v}_{f_{j+1/2}}^{n-1/2}\right)\right] \tag{4}$$

for current at $j = 0, \cdots, N-1$, and

$$\mathbf{v}_j^{n+1} = \left(\frac{C}{\Delta t} + \frac{G}{2}\right)^{-1}\left[\left(\frac{C}{\Delta t} - \frac{G}{2}\right)\mathbf{v}_j^n - \frac{1}{\Delta x}\left(\mathbf{i}_{j+1/2}^{n+1/2} - \mathbf{i}_{j-1/2}^{n+1/2}\right) + \frac{1}{2}\left(\mathbf{i}_{f_j}^{n+1} + \mathbf{i}_{f_j}^n\right)\right] \tag{5}$$

for voltage at $j = 1, \cdots, N-1$. At the near-end boundary, the voltage is updated using

$$\mathbf{v}_0^{n+1} = \left(\frac{C}{\Delta t} + \frac{G}{2} + \frac{R_{Tn}^{-1}}{\Delta x}\right)^{-1}\left[\frac{R_{Tn}^{-1}}{\Delta x}\left(\mathbf{v}_{Tn}^{n+1} + \mathbf{v}_{Tn}^n\right) + \left(\frac{C}{\Delta t} - \frac{G}{2} - \frac{R_{Tn}^{-1}}{\Delta x}\right)\mathbf{v}_0^n - \frac{2}{\Delta x}\mathbf{i}_{1/2}^{n+1/2} + \frac{1}{2}\left(\mathbf{i}_{f_0}^{n+1} + \mathbf{i}_{f_0}^n\right)\right] \tag{6}$$

Manuscript received August 6, 1996; revised March 3, 1997.

The authors are with the Department of Electrical Engineering, University of Western Ontario, London, Ont., N6A 5B9 Canada (e-mail: joe@gauss.engga.uwo.ca; tibor@gauss.engga.uwo.ca).

Publisher Item Identifier S 0018-9375(97)06304-7.

and at the far-end boundary

$$\mathbf{v}_N^{n+1} = \left(\frac{C}{\Delta t} + \frac{G}{2} + \frac{R_{Tf}^{-1}}{\Delta x}\right)^{-1}\left[\frac{R_{Tn}^{-1}}{\Delta x}\left(\mathbf{v}_{Tf}^{n+1} + \mathbf{v}_{Tf}^{n}\right) + \left(\frac{C}{\Delta t} - \frac{G}{2} - \frac{R_{Tf}^{-1}}{\Delta x}\right)\mathbf{v}_N^n + \frac{2}{\Delta x}\mathbf{i}_{N-1/2}^{n+1/2} + \frac{1}{2}\left(\mathbf{i}_{f_N}^{n+1} + \mathbf{i}_{f_N}^{n}\right)\right]. \quad (7)$$

Although these update equations are simple to use, they require a large number of points per wavelength in order to accurately represent the solution of the problem. Our intention is to develop explicit update schemes that can work with coarse space and time grids. Furthermore, for efficiency, it is very important for us to be able to run these schemes at their own stability limit. The accuracy is very much related to the choice of $\Delta t/\Delta x = \sigma$ at which the scheme is run. The *Courant* stability limit of the leapfrog scheme is given by

$$\sigma v_{\max} \leq 1$$

where $v_{\max}$ is the maximum velocity of energy propagation on the MTL. In case of a lossy MTL, the maximum velocity $v_{\max}$ must be taken as the greatest mode velocity on the *equivalent lossless* line.

It is well known that at the "*magic*" time step [6] where $\sigma v = 1$ the above leapfrog scheme gives the exact solution for *lossless homogeneous* lines where all modes propagate at the same velocity v. For this unique case, even a perfectly square wave can be exactly propagated on the grid using a relatively sparse discretization [6].

For lossless inhomogeneous lines there is more than one speed for the propagating modes and thus the *Courant* limit or "*magic*" time step can be reached only for the mode traveling with the maximum velocity. In this case, the leapfrog scheme requires a fine discretization for an accurate solution. The slower modes tend to propagate with a significant amount of numerical dispersion [7]. For lossy lines, different frequencies, even in the same mode, propagate at different velocities, but the stability limit of the leapfrog scheme is still governed by the *maximum possible* velocity on the line which, as mentioned earlier, is the velocity on the same line when the losses are set to zero.

In this paper, we derive first and second order accurate upwind schemes which allow a coarser grid to be used. This is of great advantage when one requires these schemes for solving MTL networks containing many MTL's [8]. In fact, the computer resource question only becomes an issue for large networks, but the efficient solution of large networks is becoming increasingly important in the industry [9], [10].

II. Characteristic Decomposition or "Flux" Splitting

In order to derive the new upwind schemes, the MTL equations in (1) can be written as

$$\mathbf{u}_t + A\mathbf{u}_x + B\mathbf{u} = \mathbf{0} \quad (8)$$

where $\mathbf{u}(x,t)$ is the generalized solution vector, defined as

$$\mathbf{u} = \begin{pmatrix}\mathbf{v}\\ \mathbf{i}\end{pmatrix}$$

and the matrices A and B are identified as

$$A = \begin{pmatrix}0 & C^{-1}\\ L^{-1} & 0\end{pmatrix} \quad B = \begin{pmatrix}C^{-1}G & 0\\ 0 & L^{-1}R\end{pmatrix}.$$

Letting Λ be the diagonal matrix consisting of the eigenvalues of A. It can be split up into two other matrices [7], [11], each containing only the positive and negative eigenvalues

$$\Lambda = \Lambda^- + \Lambda^+ \quad (9)$$

where

$$\Lambda^- = \begin{pmatrix}\lambda^- & 0\\ 0 & 0\end{pmatrix}, \quad \Lambda^+ = \begin{pmatrix}0 & 0\\ 0 & \lambda^+\end{pmatrix}.$$

Each eigenvalue of A represents a mode velocity in which waves are propagating to the right and left, right being the positive direction.

Let Φ and Ψ denote the right and left eigenvector matrices of A, respectively, so that $\Psi = \Phi^{-1}$, $\Psi A \Phi = \Lambda$. From these relations, A can be split as

$$\begin{aligned} A &= \Phi\Lambda\Phi^{-1}\\ &= \Phi(\Lambda^- + \Lambda^+)\Phi^{-1}\\ &= \Phi\Lambda^-\Phi^{-1} + \Phi\Lambda^+\Phi^{-1}\\ &= A^- + A^+. \end{aligned} \quad (10)$$

A new characteristic variable, $\mathbf{w}(x,t)$, can be defined as

$$\mathbf{w} = \begin{pmatrix}\mathbf{w}^-\\ 0\end{pmatrix} + \begin{pmatrix}0\\ \mathbf{w}^+\end{pmatrix} = \Psi\mathbf{u} \quad (11)$$

where we also have

$$\mathbf{u} = \Phi\mathbf{w} \quad (12)$$

and $\mathbf{w}^-$ and $\mathbf{w}^+$ represent the left and right propagating wave characteristic variables, respectively.

Using these new variables, the MTL equation (8) can be written in partially decoupled form as

$$\mathbf{w}_t + \Lambda\mathbf{w}_x = -\Psi B\Phi\mathbf{w} \quad (13)$$

whereas in terms of the original solution vector we can write

$$\mathbf{u}_t + (A^- + A^+)\mathbf{u}_x = -B\mathbf{u}. \quad (14)$$

This last equation, in which the positive and negative "fluxes" are split, is the appropriate form which we will discretize using upwind differencing techniques. The characteristic equation (13) will be used for the boundary conditions.

III. Upwind Schemes

In this section, first order and second order accurate upwind differencing techniques are presented. The general theory related to the consistency, convergence and stability of generic upwind numerical schemes can be found in [12]–[14] and is not treated here.

A. First Order Scheme

A first order scheme is obtained by simply discretizing (14) such that for the left and right propagating waves forward and backward spatial difference operators are applied, respectively. At the same time, for the loss term $B\mathbf{u}$ the trapezoidal rule is employed. We let $\sigma = \Delta t/\Delta x$ and obtain

$$\mathbf{u}_j^{n+1} = \mathbf{u}_j^n - \sigma\big(A^+\nabla\mathbf{u}_j^n + A^-\Delta\mathbf{u}_j^n\big) - \frac{1}{2}\Delta t B\big(\mathbf{u}_j^n + \mathbf{u}_j^{n+1}\big) \tag{15}$$

in which ∇ and Δ denote backward and forward spatial difference operators. By expanding the spatial operators and rearranging the above equation, we arrive at the explicit scheme given by

$$\mathbf{u}_j^{n+1} = \left(\mathbf{1} + \frac{\Delta t}{2}B\right)^{-1}\left\{\left(\mathbf{1} - \frac{\Delta t}{2}B\right)\mathbf{u}_j^n - \sigma\big[A^+\big(\mathbf{u}_j^n - \mathbf{u}_{j-1}^n\big) + A^-\big(\mathbf{u}_{j+1}^n - \mathbf{u}_j^n\big)\big]\right\}. \tag{16}$$

Note that in this scheme the discretized voltage and current vectors are *collocated* at each grid point and *not interlaced*. Also note that this is a one time-step scheme having a *Courant* stability limit of $\sigma v_{\max} \leq 1$.

B. Second Order Scheme

Warming and Beam [13] modified the corrector of the well known MacCormack scheme so that the whole scheme becomes second order accurate. This scheme was further developed by Steger and Warming [11] by incorporating the flux splitting technique.

Steger and Warming's procedure is a two step, predictor-corrector scheme. Applying it to the MTL equation (14) by simply employing the trapezoidal rule for the lossy term in both the predictor and corrector, we find

$$\begin{cases} \overline{\mathbf{u}_j^{n+1}} = \mathbf{u}_j^n - \sigma\big[A^+\nabla\mathbf{u}_j^n + A^-\Delta\mathbf{u}_j^n\big] \\ \qquad\qquad -\frac{1}{2}B\Delta t\big(\mathbf{u}_j^n + \overline{\mathbf{u}_j^{n+1}}\big) \\ \mathbf{u}_j^{n+1} = \frac{1}{2}\big(\mathbf{u}_j^n + \overline{\mathbf{u}_j^{n+1}}\big) \\ \qquad\qquad -\frac{\sigma}{2}A^+\big(\nabla\overline{\mathbf{u}_j^{n+1}} - \nabla^2\mathbf{u}_j^n\big) \\ \qquad\qquad -\frac{\sigma}{2}A^-\big(\Delta\overline{\mathbf{u}_j^{n+1}} - \Delta^2\mathbf{u}_j^n\big) \\ \qquad\qquad\quad -\frac{1}{2}\Delta t B\big(\mathbf{u}_j^{n+1} + \mathbf{u}_j^n\big). \end{cases} \tag{17}$$

If we rearrange these two equations we arrive at the following explicit scheme

$$\begin{cases} \overline{\mathbf{u}_j^{n+1}} = \big(\mathbf{1} + \frac{\Delta t}{2}B\big)^{-1}\big\{\big(\mathbf{1} - \frac{\Delta t}{2}B\big)\mathbf{u}_j^n \\ \qquad -\sigma\big[A^+\big(\mathbf{u}_j^n - \mathbf{u}_{j-1}^n\big) + A^-\big(\mathbf{u}_{j+1}^n - \mathbf{u}_j^n\big)\big]\big\} \\ \mathbf{u}_j^{n+1} = \big(\mathbf{1} + \frac{\Delta t}{2}B\big)^{-1}\frac{1}{2}\big[\big(\mathbf{u}_j^n + \overline{\mathbf{u}_j^{n+1}}\big) \\ \qquad -\sigma A^+\big(\overline{\mathbf{u}_j^{n+1}} - \overline{\mathbf{u}_{j-1}^{n+1}} + \mathbf{u}_j^n - 2\mathbf{u}_{j-1}^n + \mathbf{u}_{j-2}^n\big) \\ \qquad -\sigma A^-\big(\overline{\mathbf{u}_{j+1}^{n+1}} - \mathbf{u}_j^{n+1} - \mathbf{u}_{j+2}^n + 2\mathbf{u}_{j+1}^n - \mathbf{u}_j^n\big) \\ \qquad\qquad -\Delta t B\mathbf{u}_j^n\big]. \end{cases} \tag{18}$$

The advantage of this scheme is that the *Courant* number is 2, i.e. in order to maintain the stability the condition $v_{\max}\sigma \leq 2$ must be satisfied. However, the accuracy obtained with this simple use of the trapezoidal rule to take care of the loss term is not very good and a slight modification is required.

Another difficulty arises in the formulation of the boundary conditions since the numerical stencil is 5 nodes wide in space. In other words in order to calculate $\mathbf{u}_j^{n+1}$ the scheme makes use of $\mathbf{u}_{j+i}^n$ where $i = -2, \cdots, 2$. Modifications in order to incorporate *Thévenin* boundary conditions and increase the accuracy of modeling the loss term $B\mathbf{u}$ will now be discussed.

IV. Incorporation of Boundary Conditions

The accurate discretization of the boundary conditions given by (2) and (3) for incorporation into both upwind schemes will now be discussed. The resulting formulation is exact in the case of a *homogeneous lossless* line and it is a good approximation in the case of *lossy* transmission lines.

A. First Order Scheme

By making use of the characteristic variable $\mathbf{w}$ defined in Section II, we can write (2) at time step $n+1$ as

$$(\mathbf{1} \quad R_{Tn})\Phi\mathbf{w}_0^{n+1} = \mathbf{v}_{Tn}^{n+1} \tag{19}$$

where $\mathbf{v}_{Tn}^{n+1}$ is known.

Letting

$$\Theta_n = (\mathbf{1} \quad R_{Tn})\Phi = (\Theta_{n_1} \quad \Theta_{n_2}) \tag{20}$$

where Θ_{n_1} and Θ_{n_2} are $M \times M$ matrices, we can rewrite (19) as

$$\Theta_{n_1}\mathbf{w}_0^{-^{n+1}} + \Theta_{n_2}\mathbf{w}_0^{+^{n+1}} = \mathbf{v}_{Tn}^{n+1}. \tag{21}$$

Assuming for now that the transmission line is *lossless* and $\sigma v = 1$, we have the exact relationship

$$\mathbf{w}_0^{-^{n+1}} = \mathbf{w}_1^{-^n} \tag{22}$$

and we can write

$$\mathbf{w}_0^{+^{n+1}} = \Theta_{n_2}^{-1}\big(\mathbf{v}_{Tn}^{n+1} - \Theta_{n_1}\mathbf{w}_1^{-^n}\big). \tag{23}$$

The characteristic variable $\mathbf{w}_1^{-^n}$ is related to $\mathbf{u}_1^n$ by

$$\mathbf{w}_1^{-^n} = (\Psi_{11} \quad \Psi_{12})\mathbf{u}_1^n \tag{24}$$

where Ψ_{11} and Ψ_{12} are block matrices found from

$$\Psi = \begin{pmatrix} \Psi_{11} & \Psi_{12} \\ \Psi_{21} & \Psi_{22} \end{pmatrix} = \Phi^{-1}. \tag{25}$$

At the boundary, once the characteristic variable $\mathbf{w}_0^{+^{n+1}}$ is calculated using (23) the voltage and the current can then be obtained from the transformation

$$\mathbf{u}_0^{n+1} = \Phi\begin{pmatrix} \mathbf{w}_0^{-^{n+1}} \\ \mathbf{w}_0^{+^{n+1}} \end{pmatrix} = \Phi\begin{pmatrix} \mathbf{w}_1^{-^n} \\ \mathbf{w}_0^{+^{n+1}} \end{pmatrix} \tag{26}$$

or, more explicitly

$$\mathbf{u}_0^{n+1} = \Phi\begin{pmatrix} \mathbf{w}_1^{-^n} \\ \Theta_{n_2}^{-1}\big(\mathbf{v}_{Tn}^{n+1} - \Theta_{n_1}\mathbf{w}_1^{-^n}\big) \end{pmatrix} \tag{27}$$

where $\mathbf{w}_1^{-^n}$ is given by (24).

At the far-end similar equations can be found. These are

$$\mathbf{u}_N^{n+1} = \Phi\begin{pmatrix} \Theta_{f_1}^{-1}\big(\mathbf{v}_{Tf}^{n+1} - \Theta_{f_2}\mathbf{w}_{N-1}^{+^n}\big) \\ \mathbf{w}_{N-1}^{+^n} \end{pmatrix} \tag{28}$$

where we have used the fact that $\mathbf{w}_N^{+^{n+1}} = \mathbf{w}_{N-1}^{+^n}$ and $\Theta_f = (\Theta_{f_1} \quad \Theta_{f_2}) = (\mathbf{1} \quad -R_{Tf})\Phi$.

The first order upwind method consists of updating all interior points of the MTL using (16) and updating the end points using (27) and (28). Although (27) and (28) do not include contributions due to losses, numerical experiments have shown the effect to be negligible.

B. Second Order Scheme—Lossless Lines

As it has been pointed out in Section III-B, the second order scheme (18) uses $\mathbf{u}_{j-2}^n, \cdots, \mathbf{u}_{j+2}^n$ to calculate $\mathbf{u}_j^{n+1}$. Since at the near-end boundary $\mathbf{u}_{-2}^n$ and $\mathbf{u}_{-1}^n$ and, at the far-end, $\mathbf{u}_{N+1}^n$ and $\mathbf{u}_{N+2}^n$ are "nonexistent," we make use of the boundary condition formulation (27) and (28) as follows. First, calculate $\mathbf{u}_0^{n+1/2}$, $\mathbf{u}_1^{n+1/2}$, $\mathbf{u}_{N-1}^{n+1/2}$ and $\mathbf{u}_N^{n+1/2}$, and then, we can calculate $\mathbf{u}_0^{n+1}$ and $\mathbf{u}_N^{n+1}$ from $\mathbf{u}_1^{n+1/2}$, $\mathbf{u}_{N-1}^{n+1/2}$ using the boundary conditions again. The interior values $\mathbf{u}_1^{n+1}$ and $\mathbf{u}_{N-1}^{n+1}$ are determined using the predictor equation of the scheme and field values at time step $n+1/2$. Once again, the formulation is exact, but only in the *homogeneous lossless* case.

First, let us take a look at a *homogeneous lossless* line in which the MTL equations are written as

$$\mathbf{u}_t + A\mathbf{u}_x = \mathbf{0}.$$

The "fluxes" can be split so that (see Section II) we obtain

$$\mathbf{u}_t + (A^+ + A^-)\mathbf{u}_x = \mathbf{0}.$$

The predictor of the Steger and Warming method [11] is written as

$$\mathbf{u}_j^{\overline{n+1}} = \mathbf{u}_j^n - \sigma\left[\nabla\left(\mathbf{f}_j^{+^n}\right) + \Delta\left(\mathbf{f}_j^{-^n}\right)\right] \tag{29}$$

where $\mathbf{f}^+ = A^+\mathbf{u}$ and $\mathbf{f}^- = A^-\mathbf{u}$ are the "fluxes." We rewrite (29) as

$$\mathbf{u}_j^{\overline{n+1}} = \mathbf{u}_j^n + \sigma\left[S_-\left(\mathbf{f}_j^{+^n}\right) - S_+\left(\mathbf{f}_j^{-^n}\right) - \mathbf{f}_j^{+^n} + \mathbf{f}_j^{-^n}\right] \tag{30}$$

where the finite difference shift operators are defined as

$$S_-(\mathbf{v}_j) = \mathbf{v}_{j-1} \quad \text{and} \quad S_+(\mathbf{v}_j) = \mathbf{v}_{j+1}.$$

It is not difficult to show that

$$-\mathbf{f}_j^{+^n} + \mathbf{f}_j^{-^n} = -|\Lambda|\mathbf{u}_j^n \tag{31}$$

and that, therefore, (30) can also be written as

$$\mathbf{u}_j^{\overline{n+1}} = \mathbf{u}_j^n + \sigma\left[S_-\left(\mathbf{f}_j^{+^n}\right) - S_+\left(\mathbf{f}_j^{-^n}\right) - |\Lambda|\mathbf{u}_j^n\right]. \tag{32}$$

The exact solution at $n+1/2$ is given by

$$\mathbf{u}_j^{n+1/2} = \frac{\sigma}{2}\left[S_-\left(\mathbf{f}_j^{+^n}\right) - S_+\left(\mathbf{f}_j^{-^n}\right)\right] \tag{33}$$

where $v\Delta t/\Delta x = 2$. Now, from (32) and (33) we conclude that

$$\begin{aligned}\mathbf{u}_j^{\overline{n+1}} &= \mathbf{u}_j^n + 2\mathbf{u}_j^{n+1/2} - 2\mathbf{u}_j^n \\ &= -\mathbf{u}_j^n + 2\mathbf{u}_j^{n+1/2}.\end{aligned} \tag{34}$$

By making use of this final result the following method is found to deal with the boundary conditions (2) and (3).

1) Calculate $\mathbf{u}_j^{\overline{n+1}}$, $j = 1, \cdots, N-1$ using the predictor of (18).
2) Use (27) and (28) to determine $\mathbf{u}_0^{n+1/2}$ and $\mathbf{u}_N^{n+1/2}$, respectively.
3) Employ (34) to find the exact values $\mathbf{u}_j^{n+1/2}$, $j \in \{1, 2, N-2, N-1\}$.
4) Use (27) and (28) to determine $\mathbf{u}_0^{n+1}$ and $\mathbf{u}_N^{n+1}$, respectively, since $\mathbf{u}_1^{n+1/2}$ and $\mathbf{u}_{N-1}^{n+1/2}$ are now known.
5) Determine $\mathbf{u}_j^{n+1}$, $j \in \{1, N-1\}$ using the predictor of (18) and (34).
6) Finally, use the corrector of the second order scheme (18) to calculate the rest of the $\mathbf{u}_j^{n+1}$, i.e. for $j = 2, \cdots, N-2$.

This scheme works well for *lossless* lines and is in fact exact for *lossless homogeneous* lines. Unfortunately, this method does not work well *if the line is lossy*. That is, by simply adding loss terms using the trapezoidal rule, the scheme does not give good results. In order to fix this problem, we create another slightly modified algorithm which is presented in the next section.

V. Second Order Upwind Scheme—Lossy Lines

Numerical results have shown that the previously mentioned second order scheme has problems with the integration of the lossy term. Therefore the following scheme has been derived which handles lossy lines as well. Let us consider the Steger and Warming [11] scheme in case of a lossless line, i.e.,

$$\begin{cases} \mathbf{u}_j^{\overline{n+1}} = \mathbf{u}_j^n - \sigma\left[A^+\nabla\mathbf{u}_j^n + A^-\Delta\mathbf{u}_j^n\right] \\ \mathbf{u}_j^{n+1} = \frac{1}{2}\left(\mathbf{u}_j^n + \mathbf{u}_j^{\overline{n+1}}\right) \\ \qquad\qquad - \frac{\sigma}{2}A^+\left(\nabla\mathbf{u}_j^{\overline{n+1}} - \nabla^2\mathbf{u}_j^n\right) \\ \qquad\qquad - \frac{\sigma}{2}A^-\left(\Delta\mathbf{u}_j^{\overline{n+1}} - \Delta^2\mathbf{u}_j^n\right). \end{cases} \tag{35}$$

From (35) and (34) this scheme can be written as

$$\begin{cases} \mathbf{u}_j^{n+1/2} = \mathbf{u}_j^n - \frac{\sigma}{2}\left(A^+\nabla\mathbf{u}_j^n + A^-\Delta\mathbf{u}_j^n\right) \\ \mathbf{u}_j^{\overline{n+1}} = 2\mathbf{u}_j^{n+1/2} - \mathbf{u}_j^n \\ \mathbf{u}_j^{n+1} = \mathbf{u}_j^{n+1/2} - \frac{\sigma}{2}A^+\left(\nabla\mathbf{u}_j^{\overline{n+1}} - \nabla^2\mathbf{u}_j^n\right) \\ \qquad\qquad - \frac{\sigma}{2}A^-\left(\Delta\mathbf{u}_j^{\overline{n+1}} - \Delta^2\mathbf{u}_j^n\right). \end{cases} \tag{36}$$

Now we add the loss term using the trapezoidal method to arrive at

$$\begin{cases} \mathbf{u}_j^{n+1/2} = \mathbf{u}_j^n - \frac{\sigma}{2}\left(A^+\nabla\mathbf{u}_j^n + A^-\Delta\mathbf{u}_j^n\right) \\ \qquad\qquad - \frac{1}{2}\frac{\Delta t}{2}B\left(\mathbf{u}_j^n + \mathbf{u}_j^{n+1/2}\right) \\ \mathbf{u}_j^{\overline{n+1}} = 2\mathbf{u}_j^{n+1/2} - \mathbf{u}_j^n \\ \mathbf{u}_j^{n+1} = \mathbf{u}_j^{n+1/2} - \frac{\sigma}{2}A^+\left(\nabla\mathbf{u}_j^{\overline{n+1}} - \nabla^2\mathbf{u}_j^n\right) \\ \qquad\qquad - \frac{\sigma}{2}A^-\left(\Delta\mathbf{u}_j^{\overline{n+1}} - \Delta^2\mathbf{u}_j^n\right) \\ \qquad\qquad - \frac{1}{2}\frac{\Delta t}{2}B\left(\mathbf{u}_j^{n+1} + \mathbf{u}_j^{n+1/2}\right) \end{cases} \tag{37}$$

and rearrange these to get

$$\begin{cases} \mathbf{u}_j^{n+1/2} = \left(1 + \frac{\Delta t}{4}B\right)^{-1}\left[\left(1 - \frac{\Delta t}{4}B\right)\mathbf{u}_j^n \right. \\ \qquad\qquad \left. - \frac{\sigma}{2}\left(A^+\nabla\mathbf{u}_j^n + A^-\Delta\mathbf{u}_j^n\right)\right] \\ \mathbf{u}_j^{\overline{n+1}} = 2\mathbf{u}_j^{n+1/2} - \mathbf{u}_j^n \\ \mathbf{u}_j^{n+1} = \left(1 + \frac{\Delta t}{4}B\right)^{-1}\left[\left(1 - \frac{\Delta t}{4}B\right)\mathbf{u}_j^{n+1/2}\right. \\ \qquad\qquad - \frac{\sigma}{2}A^+\left(\nabla\mathbf{u}_j^{\overline{n+1}} - \nabla^2\mathbf{u}_j^n\right) \\ \qquad\qquad \left. - \frac{\sigma}{2}A^-\left(\Delta\mathbf{u}_j^{\overline{n+1}} - \Delta^2\mathbf{u}_j^n\right)\right]. \end{cases} \tag{38}$$

Since at the *Courant* stability limit of 2 of this scheme the relationship between Δt and Δx is

$$\frac{\Delta t}{\Delta x} = \frac{2}{v_{\max}}. \tag{39}$$

It follows that, under the same spatial discretization conditions, the underlying Δt in (38) is double the value of that in (27) or (28). Therefore, we rewrite (27) and (28) in order to reflect this fact

$$\mathbf{u}_0^{n+1/2} = \Phi\begin{pmatrix} \mathbf{w}_1^{-^n} \\ \Theta_{n_2}^{-1}\left(\mathbf{v}_{Tn}^{n+1/2} - \Theta_{n_1}\mathbf{w}_1^{-^n}\right) \end{pmatrix} \tag{40}$$

and

$$\mathbf{u}_N^{n+1/2} = \Phi\begin{pmatrix} \Theta_{f_1}^{-1}\left(\mathbf{v}_{Tf}^{n+1/2} - \Theta_{f_2}\mathbf{w}_{N-1}^{+^n}\right) \\ \mathbf{w}_{N-1}^{+^n} \end{pmatrix} \tag{41}$$

in which $\mathbf{w}_{N-1}^{+^n}$ is defined similarly to $\mathbf{w}_1^{-^n}$ which in turn is given by (24). Another needed form of (40) and (41) is when we write them to calculate $\mathbf{u}_0^{n+1}$ and $\mathbf{u}_N^{n+1}$. These are

$$\mathbf{u}_0^{n+1} = \Phi\begin{pmatrix} \mathbf{w}_1^{-^{n+1/2}} \\ \Theta_{n_2}^{-1}\left(\mathbf{v}_{Tn}^{n+1} - \Theta_{n_1}\mathbf{w}_1^{-^{n+1/2}}\right) \end{pmatrix} \tag{42}$$

and

$$\mathbf{u}_N^{n+1} = \Phi\begin{pmatrix} \Theta_{f_1}^{-1}\left(\mathbf{v}_{Tf}^{n+1} - \Theta_{f_2}\mathbf{w}_{N-1}^{+^{n+1/2}}\right) \\ \mathbf{w}_{N-1}^{+^{n+1/2}} \end{pmatrix} \tag{43}$$

in which $\mathbf{w}_1^{-^{n+1/2}}$ is defined as

$$\mathbf{w}_1^{-^{n+1/2}} = \begin{pmatrix} \Psi_{11} & \Psi_{12} \end{pmatrix}\mathbf{u}_1^{n+1/2}. \tag{44}$$

Equation (38) in combination with (40)–(43) constitute the update equations of the second order upwind scheme.

The final algorithm becomes the following.

1) Use (38a) to determine $\mathbf{u}_j^{n+1/2}$, $j = 1, \cdots, N-1$, and use (40) and (41) to determine $\mathbf{u}_0^{n+1/2}$ and $\mathbf{u}_N^{n+1/2}$.
2) Now that $\mathbf{u}_j^{n+1/2}$ is known for all j, use (42) and (43) to determine $\mathbf{u}_0^{n+1}$ and $\mathbf{u}_N^{n+1}$, respectively.
3) Employ (38b) to find the predicted values $\mathbf{u}_j^{\overline{n+1}}$, $j = 1, \cdots, N-1$.
4) Finally, use the corrector of (38) to calculate the rest of the $\mathbf{u}_j^{n+1}$, i.e. for $j = 2, \cdots, N-2$, and determine $\mathbf{u}_j^{n+1}$, $j \in \{1, N-1\}$ using (38a).

VI. Numerical Results

All the previously described numerical schemes have been thoroughly tested. In the following we will show the most important results we found by numerical testing. Throughout our MTL testing the lines were not necessarily matched and attention was placed on solving real life problems.

The very first case we present is a single 1.209445 m long lossy line, resolved into 34 cells (Δx) giving us $\Delta x = 35.5719$ mm. The line parameters are $L = 0.805969$ μH/m, $C = 88.2488$ pF, $R = 86.207$ Ω/m and $G = 0$ S/m, and the line is terminated on both ends in $R_{Tn} = R_{Tf} = 50$ Ω pure resistive loads.

First, we present the solutions to an initial value problem, where the initial condition has been set to a centered trapezoidal voltage pulse along the line with an amplitude of 1 V, rising- and falling-edge as wide as one Δx, i.e. 35.5719 mm and a total width of $6\Delta x$. The initial line current has been set to zero everywhere along the line. Under these circumstances, the wave splits up. The schemes are run at the *Courant* limit, i.e. $\Delta t = 0.299$ ns for the leapfrog and first order upwind schemes, and $\Delta t = 0.599$ ns for the second order upwind scheme. Fig. 1 zooms in on the left propagating wave after 3.599995 ns. We note that *the differences between the leapfrog, first order, (16), and second order, (38), upwind solutions are due to the lossy characteristic of the line, since in the lossless case there are no differences since all schemes give the exact solution*. The solution given by the first order upwind scheme differs from that of the leapfrog scheme in an overshoot at the front of the wave and undershoot at the trailing of the wave. These differences are not as severe in the case of the second order upwind scheme. However, there is another discrepancy between the second order upwind and leapfrog solutions, namely the low amplitude oscillations left behind the wave.

For the same transmission line a boundary value problem is presented next. The spatial discretization is the same as before, i.e. 34 cells ($\Delta x = 35.5719$ mm). Initial conditions are set to zero and the near-end load resistance is replaced with a *Thévenin* voltage source with an internal resistance of $R_{Tn} = 50$ Ω. The *Thévenin* voltage source is a trapezoidal pulse with a 1 V amplitude, $2\Delta t$ ($\Delta t = 0.299$ ns) rise and fall-time and is 12 ns long. From Fig. 2 we can see that the first order upwind method returns the same type of over- and undershoots as in the initial value problem. Furthermore, it is to be noted that in the second order upwind case the over- and undershoots disappear but, due to the low resolution and the lossless line formulation of the boundary conditions, the wave amplitude is a bit above its real value. These inaccuracies are peculiar to applying upwind to a single line and disappear when applying the schemes to general, N-conductor MTL's. In any case, we are not proposing to use upwind scheme for a single line where there is only one mode of propagation and the leap-frog scheme suffices.

It is interesting to see, that even at low resolution, all these differences among the three solutions vanish in the case of MTL's with more than two conductors. For example, in the case of a homogeneous lossy line with the parameters

$$\begin{aligned} &\text{Length} = 1 \text{ m} \\ &L = \begin{pmatrix} 0.747\,463\,5 & 0.507\,009\,4 \\ 0.507\,009\,4 & 1.014\,018 \end{pmatrix} \mu\text{H/m} \\ &C = \begin{pmatrix} 22.494 & -11.247 \\ -11.247 & 16.581 \end{pmatrix} \text{pF/m} \\ &R = \begin{pmatrix} 10 & 5 \\ 5 & 10 \end{pmatrix} \Omega\text{/m} \\ &G = \begin{pmatrix} 0 & 0 \\ 0 & 0 \end{pmatrix} \text{S/m} \\ &\Delta x = 5 \text{ cm}, (20 \text{ cells}) \end{aligned}$$

the *Courant* limit gives us $\Delta t = 0.166$ ns for the leapfrog and first order upwind schemes, and $\Delta t = 0.333$ ns for the second

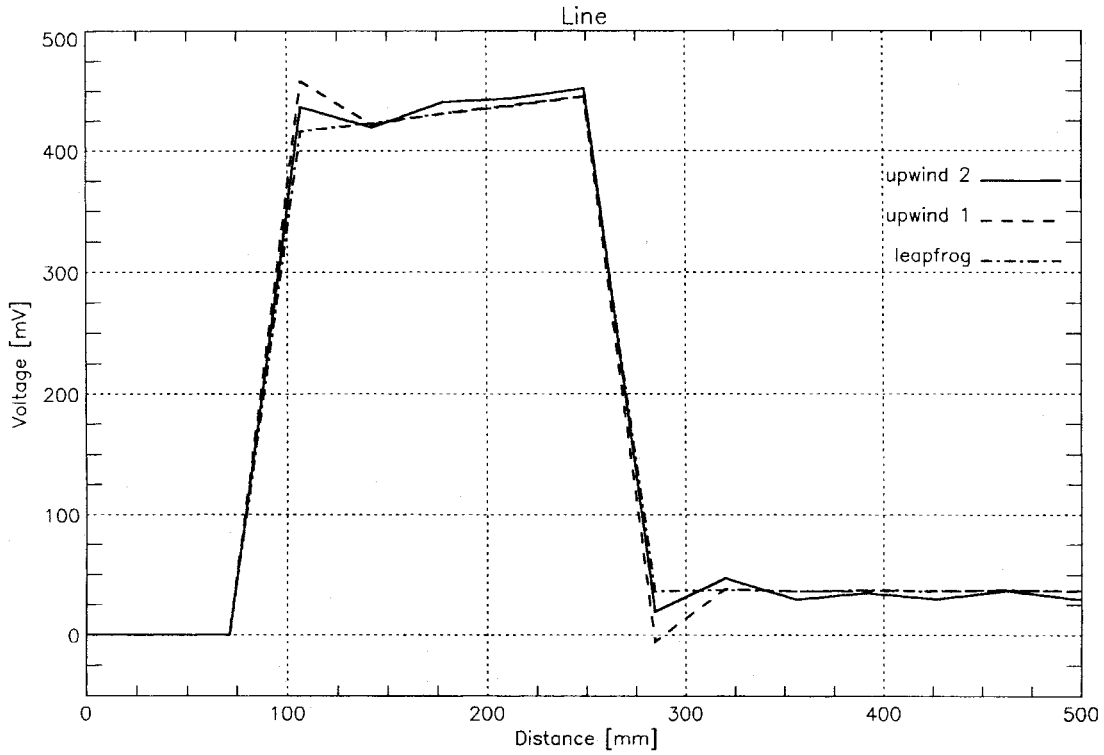

Fig. 1. Initial value problem: two-conductor line, wave propagating to the left.

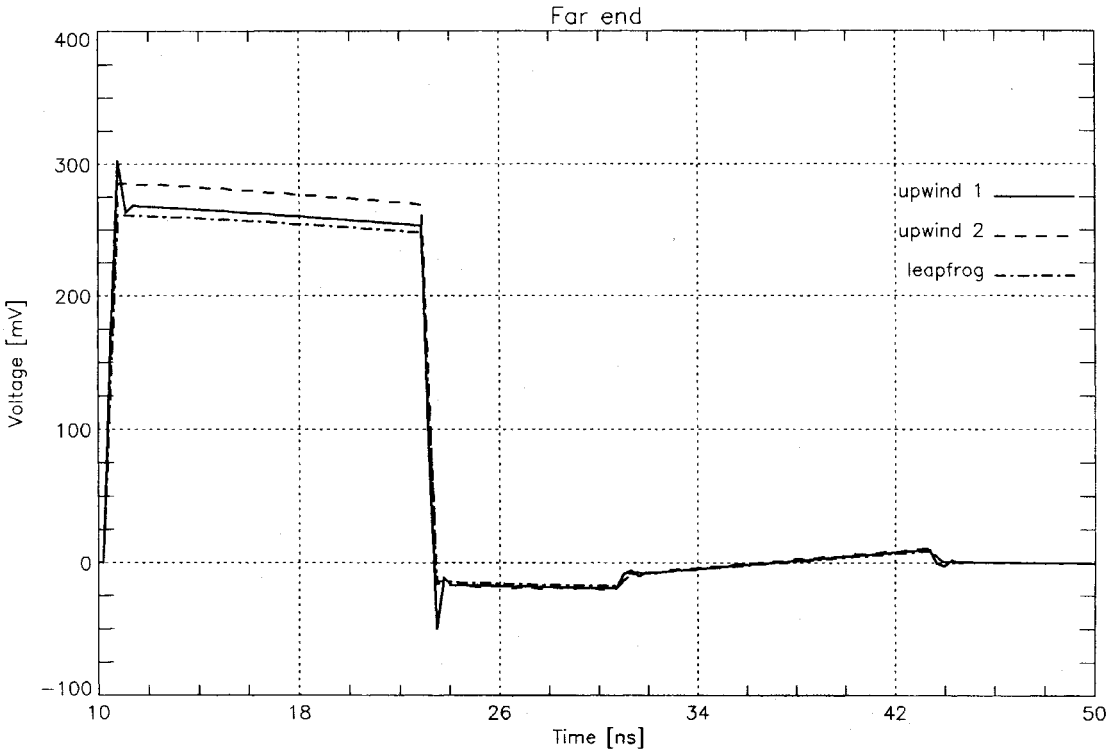

Fig. 2. Boundary value problem: two-conductor line, far end voltage.

order upwind scheme. We choose the *Thévenin* sources to be

$$R_{Tn} = R_{Tf} = \begin{pmatrix} 50 & 0 \\ 0 & 50 \end{pmatrix} \Omega$$

$$\mathbf{v}_{Tn} = \left(\begin{Bmatrix} t_r = t_f = 0.334 \text{ ns}, \\ t_p = 12.5 \text{ ns}, \quad \text{and} \quad \text{Peak} = 1 \text{ V} \end{Bmatrix} \right)$$
$$0 \text{ V}$$

and

$$\mathbf{v}_{Tf} = \begin{pmatrix} 0 \\ 0 \end{pmatrix} \text{V}$$

(t_r, t_f and t_p denote the rise-, fall- and peak-time of the trapezoidal pulse, respectively). The far-end cross-talk is found to be almost exactly the same by all three techniques (see

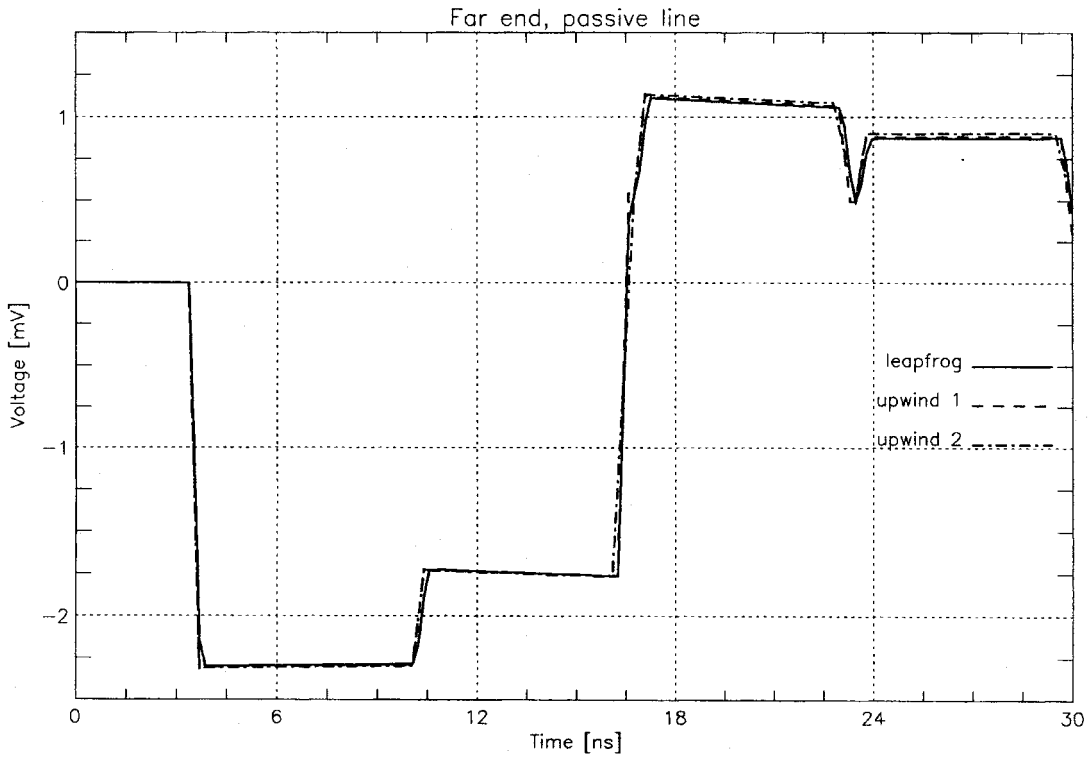

Fig. 3. Boundary value problem: three-conductor homogeneous lossy line.

Fig. 3). It is very important to note that, in all cases presented so far there has been only one modal velocity and *all schemes have been run at their Courant limit.*

The reason the upwind methods have been developed for solving MTL's is to reduce, possibly eliminate, the numerical dispersion which occurs in the leapfrog solution, when the line is inhomogeneous i.e. the different modes do not propagate with the same speed. These examples will be considered next.

Let us consider a three-conductor lossless transmission line with

$$\text{Length} = 2 \text{ m}$$
$$L = \begin{pmatrix} 5.03 & 0.1 \\ 0.1 & 10 \end{pmatrix} \mu\text{H/m}$$
$$C = \begin{pmatrix} 50 & -5 \\ -5 & 100 \end{pmatrix} \text{pF/m}.$$

The two modes of this line propagate at the speeds $v_1 = 3.16163 \times 10^7$ m/s and $v_2 = 6.32326 \times 10^7$ m/s, respectively, of which the greater value is used to find that $\Delta t = 1.581463$ ns, for the leapfrog and first order upwind schemes, and $\Delta t = 3.162\,925$ ns, for the second order upwind scheme if $\Delta x = 10$ cm (equivalent to 20 cells). We note that in this example the difference between the two modal velocities is 50%, which is a significant value.

If the terminal conditions are given by the *Thévenin* sources with the parameters

$$R_{Tn} = R_{Tf} = \begin{pmatrix} 50 & 0 \\ 0 & 50 \end{pmatrix} \Omega$$
$$\mathbf{v}_{Tn} = \begin{pmatrix} \left\{ \begin{matrix} t_r = t_f = 0.8 \text{ ns}, \\ t_p = 30 \text{ ns}, \text{ and Peak} = 1 \text{ V} \end{matrix} \right\} \\ 0 \text{ V} \end{pmatrix}$$

and

$$\mathbf{v}_{Tf} = \begin{pmatrix} 0 \\ 0 \end{pmatrix} \text{V}$$

the far-end crosstalk voltages given by the three methods are as shown in Fig. 4.

The three methods compare in a similar fashion even if the line is lossy. Such a case is displayed in Fig. 5, where a lossy characteristic of

$$R = \begin{pmatrix} 10 & 5 \\ 5 & 10 \end{pmatrix} \Omega/\text{m}$$

and

$$G = \begin{pmatrix} 0 & 0 \\ 0 & 0 \end{pmatrix} \text{S/m}$$

has been added to the line of our previous example and the same terminal conditions have been applied.

The differences between any two of the three methods are so obvious that they hardly need any comments. In case of the leapfrog scheme, the slower propagating modes introduce a very significant amount of numerical dispersion, which is not the case in any of the upwind schemes. From these comparative plots one can also see that the second order upwind scheme has a superior accuracy to that of first order upwind scheme.

By increasing the rise- and fall-time of the imput pulse to $t_r = t_f = 3.2$ ns, thereby making the pulse more realistic, we obtain the results shown in Figs. 6 and 7 for the lossless and lossy cases, respectively. The conclusions in these two cases are the same as before.

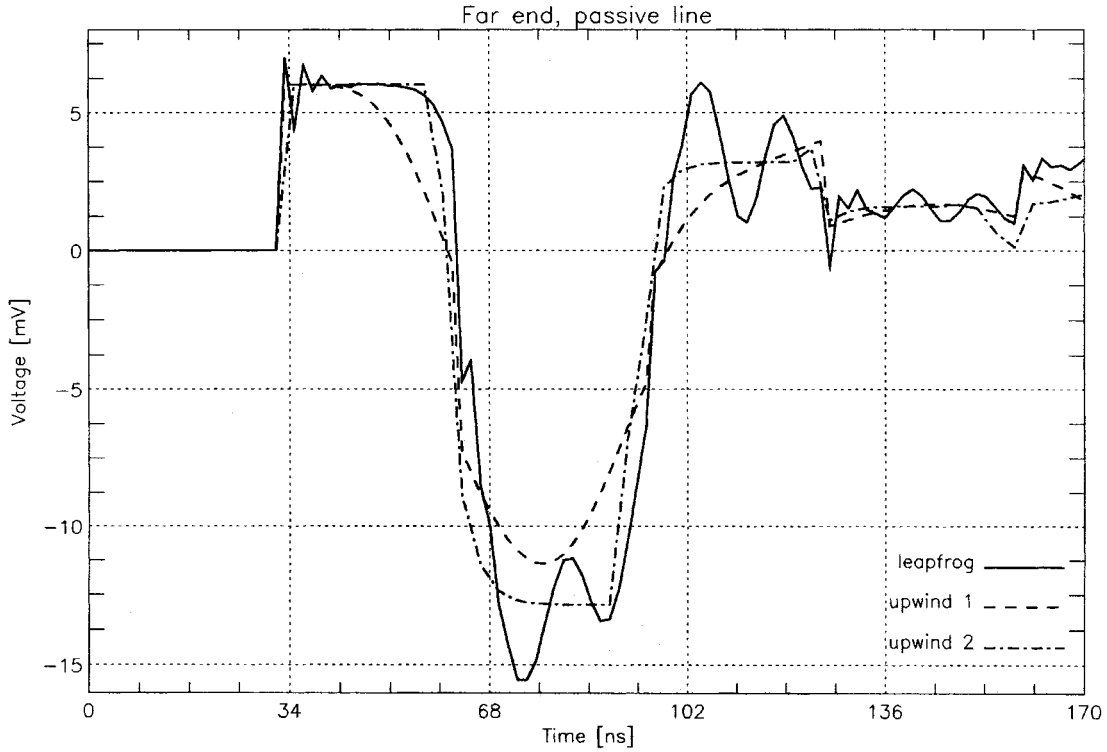

Fig. 4. Boundary value problem: three-conductor inhomogeneous lossless line ($t_r = t_f = 0.8$ ns).

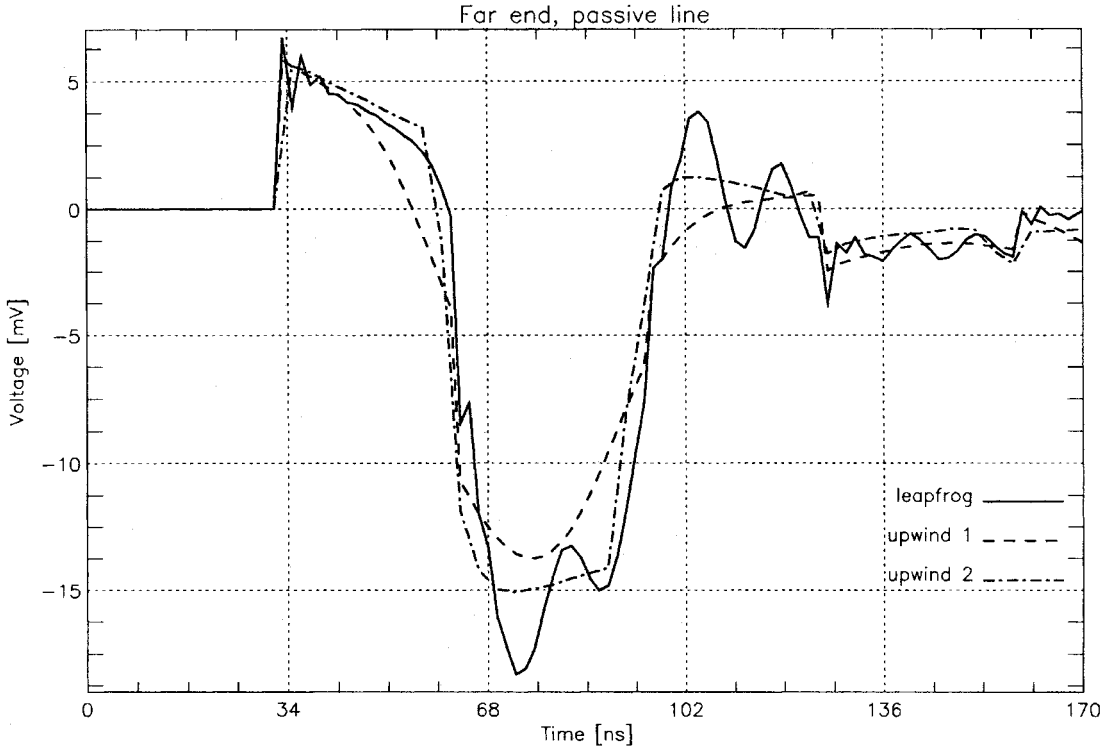

Fig. 5. Boundary value problem: three-conductor inhomogeneous lossy line ($t_r = t_f = 0.8$ ns).

It is a fascinating fact that all three schemes tend to behave similarly as the difference between the modal velocities vanishes. Such an example is given next (we have already seen that, in the case of a homogeneous MTL, where we have only one mode of propagation, the characteristics of the three schemes are extremely close to each other).

Figs. 8–11 display the far-end cross-talk occurring in a three-conductor, lossy transmission line with

$$\text{Length} = 2 \text{ m}$$

$$L = \begin{pmatrix} 0.7485 & 0.5077 \\ 0.5077 & 1.0154 \end{pmatrix} \mu\text{H/m}$$

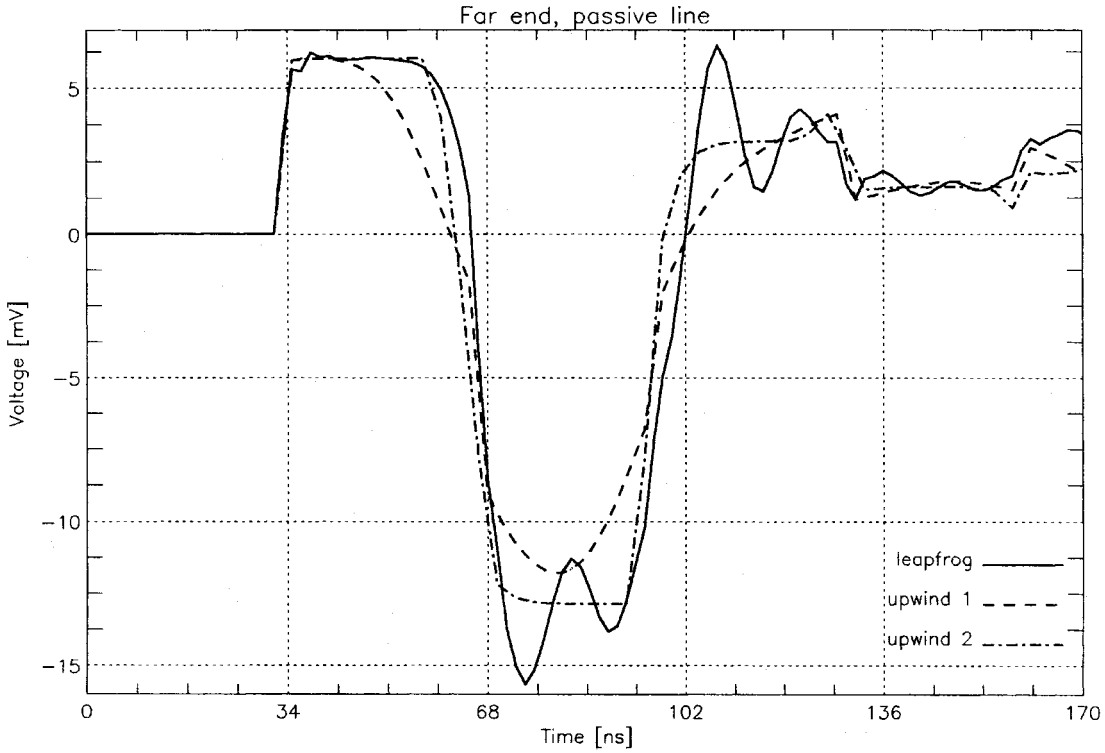

Fig. 6. Boundary value problem: three-conductor inhomogeneous lossless line ($t_r = t_f = 3.2$ ns).

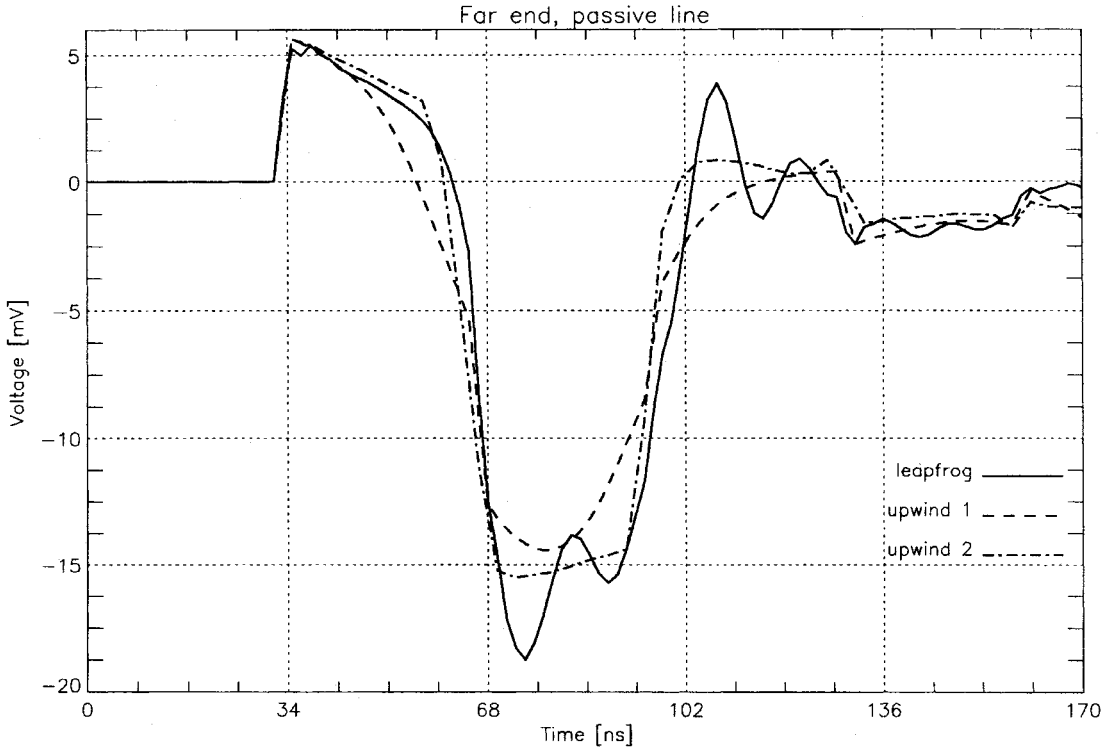

Fig. 7. Boundary value problem: three-conductor inhomogeneous lossy line ($t_r = t_f = 3.2$ ns).

$$C = \begin{pmatrix} 37.432 & -18.716 \\ -18.716 & 24.982 \end{pmatrix} \text{ pF/m}$$

$$R = \begin{pmatrix} 10 & 5 \\ 5 & 10 \end{pmatrix} \ \Omega\text{/m}$$

$$G = \begin{pmatrix} 14.1115 & -7.0558 \\ -7.0558 & 9.418 \end{pmatrix} \ \mu\text{S/m}$$

$$\epsilon_r' = 3, \quad \text{and}$$
$$\sigma = 10^{-5} \text{ S/m}.$$

By choosing a spatial discretization of 20 cells ($\Delta x = 10$ cm), at the *Courant* limit we find that for the leapfrog and the first order upwind schemes $\Delta t = 0.3983$ ns, whereas for the second order upwind scheme $\Delta t = 0.7966$ ns. The *Thévenin*

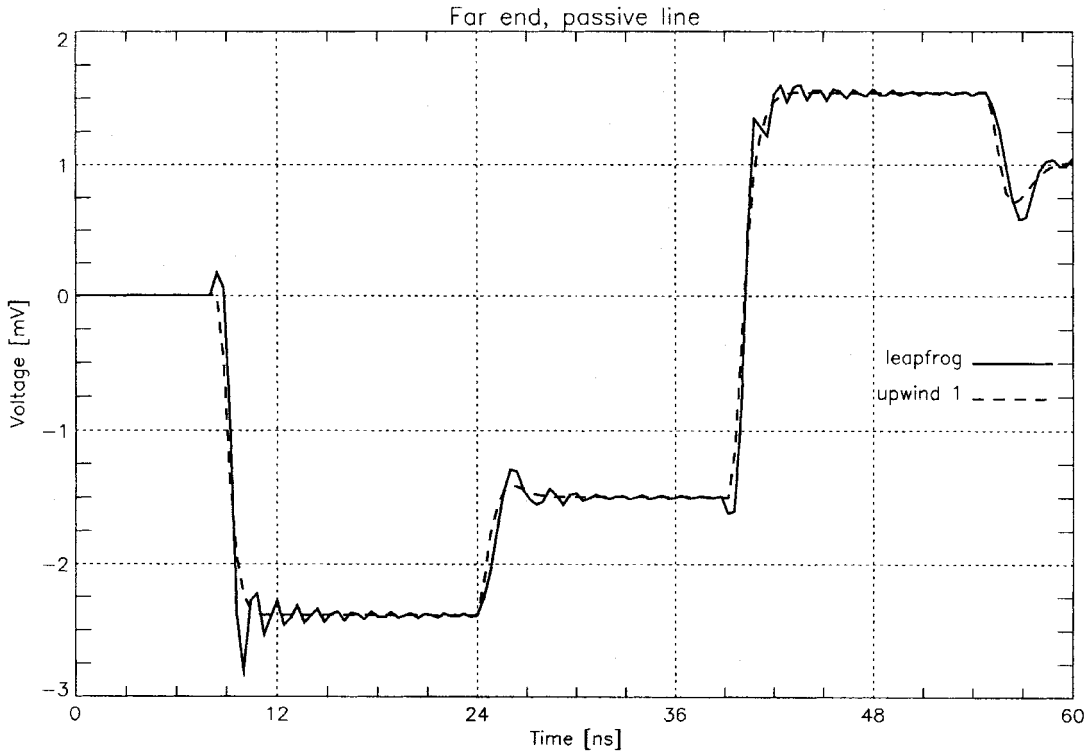

Fig. 8. Comparison of boundary value problems formulated with first order upwind and leapfrog methods: three-conductor lossless ribbon cable.

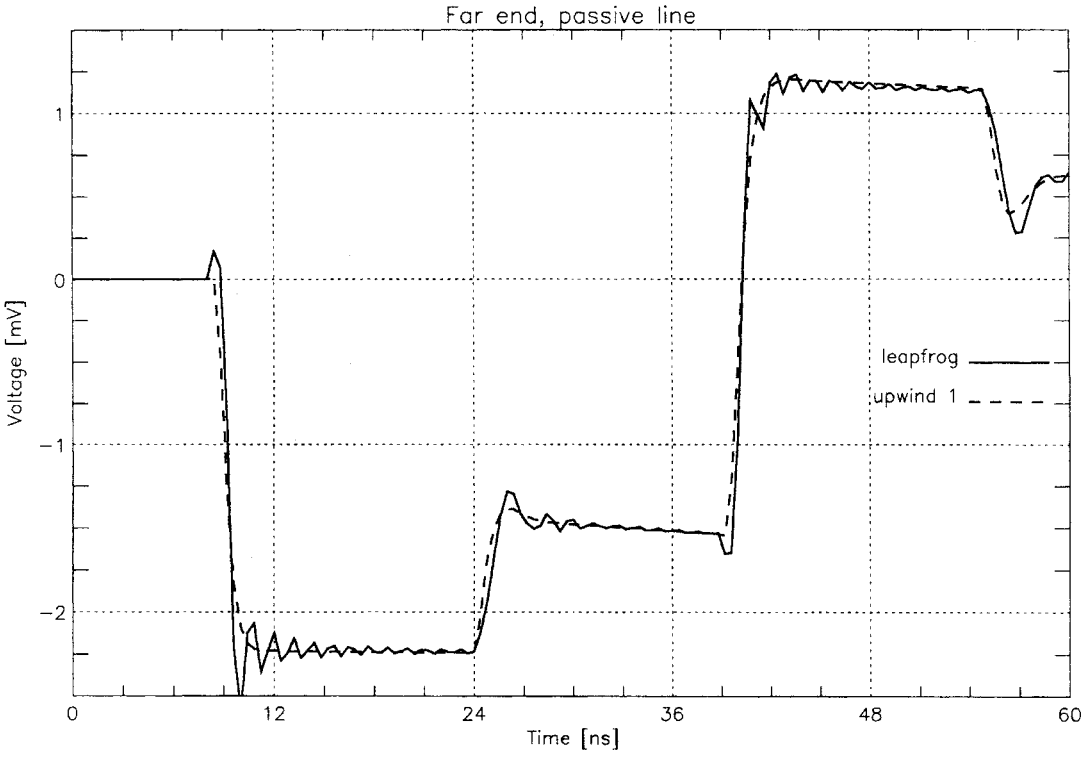

Fig. 9. Comparison of boundary value problems formulated with first order upwind and leapfrog methods: three-conductor lossy ribbon cable.

sources are

$$R_{Tn} = R_{Tf} = \begin{pmatrix} 50 & 0 \\ 0 & 50 \end{pmatrix} \Omega$$

$$\mathbf{v}_{Tn} = \begin{pmatrix} \left\{ \begin{matrix} t_r = t_f = 0.8 \text{ ns}, \\ t_p = 30 \text{ ns}, \text{ and Peak} = 1 \text{ V} \end{matrix} \right\} \\ 0 \text{ V} \end{pmatrix}$$

and

$$\mathbf{v}_{Tf} = \begin{pmatrix} 0 \\ 0 \end{pmatrix} \text{V}.$$

The speed of the fastest propagating mode has been determined to be $v = 2.5166 \times 10^8$ m/s. The slower speed being $2.323\,96 \times 10^8$ m/s, hence there is a relative difference of speed of 7.655%. This quite small difference of speed is

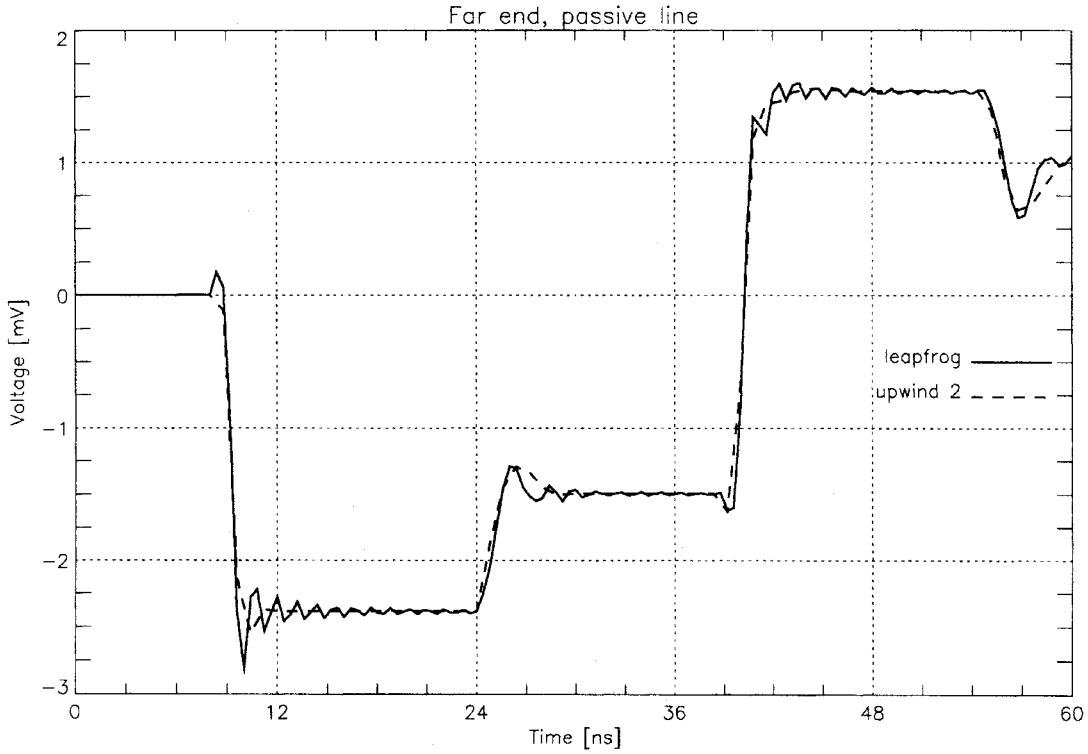

Fig. 10. Comparison of boundary value problems formulated with second order upwind and leapfrog methods: three-conductor lossless ribbon cable.

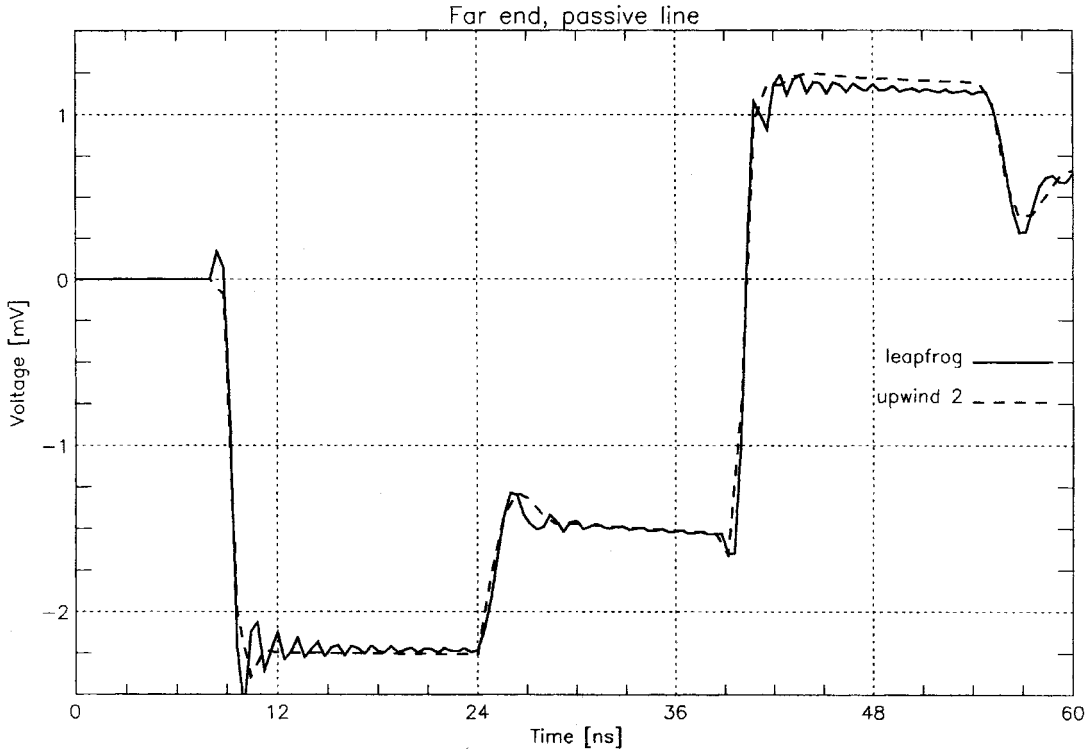

Fig. 11. Comparison of boundary value problems formulated with second order upwind and leapfrog methods: three-conductor lossy ribbon cable.

large enough for the leapfrog scheme to produce significant dispersion. This phenomenon occurs regardless of the lossy or lossless nature of the MTL.

As the test results show, the first order upwind scheme works very well for both lossless (Fig. 8) and lossy (Fig. 9) inhomogeneous lines.

Satisfactory results have been obtained with the second order upwind scheme also (Figs. 10 and 11). From these and several other test results we conclude that the second order upwind scheme follows more accurately the leapfrog solution while causing less dispersion. However, at very low resolution a tiny offset can be noticed in the amplitude of the waves which

essentially is due to the integration method of the line losses and partially is due to the approximate formulation of the boundary condition. This can be observed by comparing the lossy (see Fig. 10) and lossless (see Fig. 11) solutions of this scheme. Once again, a bit higher spatial resolution eliminates this problem.

VII. Conclusion

As it has been pointed out in [7] already, the upwind schemes have the advantage of producing significantly less dispersion than the leapfrog scheme. In addition to the formulation of the initial value problem presented in [7], a good approximation of the boundary value problem has been successfully formulated and implemented. Many test cases have been analyzed for the numerical schemes and the majority have shown the superiority of the upwind schemes in many respects (speed, numerical dispersion). An "intelligent" algorithm, which would select the most appropriate method to solve the differential equations based on the nature of the problem and the results shown in this paper is proposed. This would have the result of minimizing the number of spatial discretization points required and would lead to a much more efficient solution for MTL networks. As future work, in terms of improving the upwind schemes, the inclusion of external field coupling to transmission lines is proposed.

References

[1] C. R. Paul, *Analysis of Multiconductor Transmission Lines*. New York: Wiley, 1994.
[2] J. A. Roden, C. R. Paul, W. T. Smith, and S. D. Gedney, "Finite-difference, time-domain analysis of lossy transmission lines," *IEEE Trans. Electromag. Compat.*, vol. 38, pp. 15–24, Feb. 1996.
[3] E. M. and G. Costache, "Skin effect considerations on transient response of a line excited by an electromagnetic pulse," *IEEE Trans. Electromag. Compat.*, vol. 34, pp. 320–329, Aug. 1992.
[4] R. Siushansian and J. LoVetri, "Efficient evaluation of convolution integrals arising in FDTD formulations for electromagnetic dispersive media," in *J. Electromag. Waves Appl.*, vol. 11, pp. 101–117, 1997.
[5] A. K. Agrawal, H. J. Price, and S. H. Gurbaxani, "Transient response of multiconductor transmission lines excited by a nonuniform electromagnetic field," *IEEE Trans. Electromag. Compat.*, vol. 22, May 1980.
[6] C. R. Paul, "Incorporation of terminal constraints in the FDTD analysis of transmission lines," *IEEE Trans. Electromag. Compat.*, vol. 36, pp. 85–91, May 1994.
[7] J. LoVetri, "On characteristic based upwind differencing schemes for multiconductor transmission lines," in *Int. Symp. Electromag. Compat.*, Zurich, Switzerland, 1995, pp. 345–350.
[8] D. Mardare and J. LoVetri, "The finite-difference time-domain solution of lossy MTL networks with nonlinear junctions," *IEEE Trans. Electromag. Compat.*, vol. 37, pp. 252–259, May 1995.
[9] A. K. Goel, *High-Speed VLSI Interconnections: Modeling, Analysis and Simulation*. New York: Wiley, 1994.
[10] T. K. Tang and M. S. Nakhla, "Analysis of high-speed VLSI interconnects using the asymptotic waveform evaluation technique," *IEEE Trans. Computer-Aided Design*, vol. 11, pp. 341–352, Mar. 1992.
[11] J. L. Steger and R. F. Warming, "Flux vector splitting of the invicid gasdynamic equations with applications to finite-difference methods," *J. Comput. Phys.*, vol. 40, pp. 263–293, 1981.
[12] K. W. Morton and D. F. Mayers, *Numerical Solution of Partial Differential Equations*. Cambridge, U.K.: Cambrigde Univ. Press, 1994.
[13] R. F. Warming and R. M. Beam, "Upwind second-order difference schemes and applications in aerodynamic flows," *AIAA J.*, vol. 14, no. 9, pp. 1241–1249, Sept. 1976.
[14] B. Gustafsson, H. O. Kreiss, and J. Oliger, *Time Dependent Problems and Difference Methods*. New York: Wiley, 1995.

Joe LoVetri was born in Enna, Italy, in 1963. He received the B.Sc. (with distinction) and M.Sc. degrees, both in electrical engineering, from the University of Manitoba, Winnipeg, Man., Canada in 1984 and 1987, respectively, and the Ph.D. degree in electrical engineering from the University of Ottawa, Ottawa, Ont., Canada in 1991. .

From 1984 to 1986, he was EMI/EMC Engineer at the Sperry Defence Division, Winnipeg. From 1986 to 1988, he held the position of TEMPEST Engineer at the Communications Security Establishment, Ottawa. From 1988 to 1991, he was a Research Officer at the Institute for Information Technology, National Research Council of Canada. He is currently an Associate Professor in the Department of Electrical Engineering, The University of Western Ontario, London, where he has been since 1991. His main interests lie in time domain computational electromagnetics. His specific research interests are in time domain modeling of electromagnetic compatibility problems such as multiconductor transmission line networks and other electromagnetic interactions.

Tibor Lapohos was born in Tîrgu-Mureş, Romania, in 1967. He received the diploma in electrical engineering from the Department of Automation and Computer Technology, Polytechnic University of Cluj-Napoca, Romania, in 1991, and the M.E.Sc. degree in mechanical engineering from The University of Western Ontario, London, Ont., Canada, in 1994, where he is currently pursuing the Ph.D. degree.

His main areas of interest are time domain computational electromagnetics and electromagnetic compatibility.